eLIFE
elifesciences.org

Figures and figure supplements

Oxyntomodulin regulates resetting of the liver circadian clock by food

Dominic Landgraf, et al.

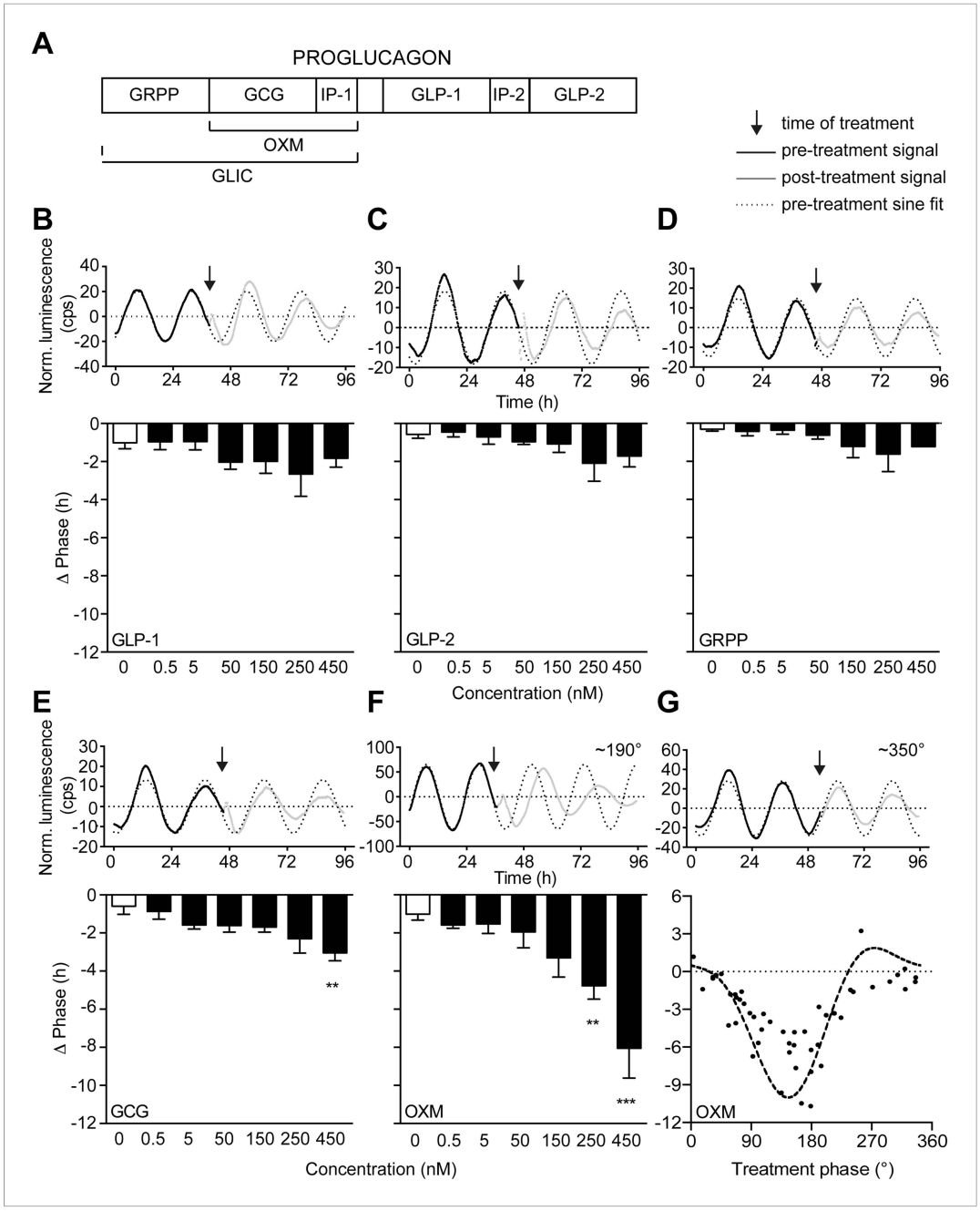

Figure 1. Oxyntomodulin (OXM) phase- and dose-dependently resets circadian clocks in liver slices. (**A**) Schematic sequence of the proglucagon-derived peptides (GRPP—glicentin-related pancreatic peptide; GLIC—glicentin; OXM—oxyntomodulin; GCG—glucagon; IP-1—intervening peptide-1; GLP-1—glucagon-like peptide-1; IP-2—intervening peptide-2; GLP-2—glucagon-like peptide-2). (**B**–**F**) Example luminescence traces and dose-dependent responses for GLP-1 (**B**; $F(6, 28) = 1.509$), GLP-2 (**C**; $F(6, 28) = 1.530$), GRPP (**D**; $F(6, 28) = 1.151$), GCG (**E**; $F(6, 28) = 3.569$), and OXM (**F**; $F(6, 28) = 8.790$)-induced phase resetting of PER2::LUC rhythms in liver slices treated at 180–200˚. Data are presented as mean ± S.E.M. (n = 5). One-way ANOVA (F-values with degrees of freedom provided in brackets): *$p < 0.05$; **$p < 0.01$; ***$p < 0.001$. Asterisks indicate significant differences relative to PBS treatment (white bars). (**G**) Phase response curve for OXM-induced phase resetting of PER2::LUC rhythms in liver slices. Circles: raw data of individual slices; dashed line: sine wave regression with harmonics.

DOI: 10.7554/eLife.06253.003

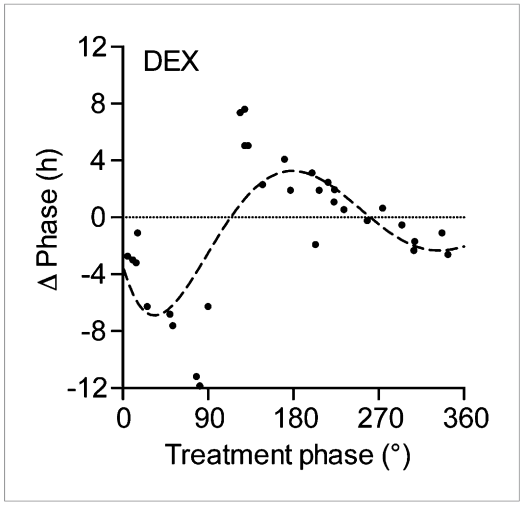

Figure 1—figure supplement 1. Phase response curve for dexamethasone (DEX) treatment in *Per2::LUC* liver slice cultures. Black dots: phase shifts of individual DEX treatments (100 μM); dashed line: sine wave regression with first and second order harmonics (CircWave).
DOI: 10.7554/eLife.06253.005

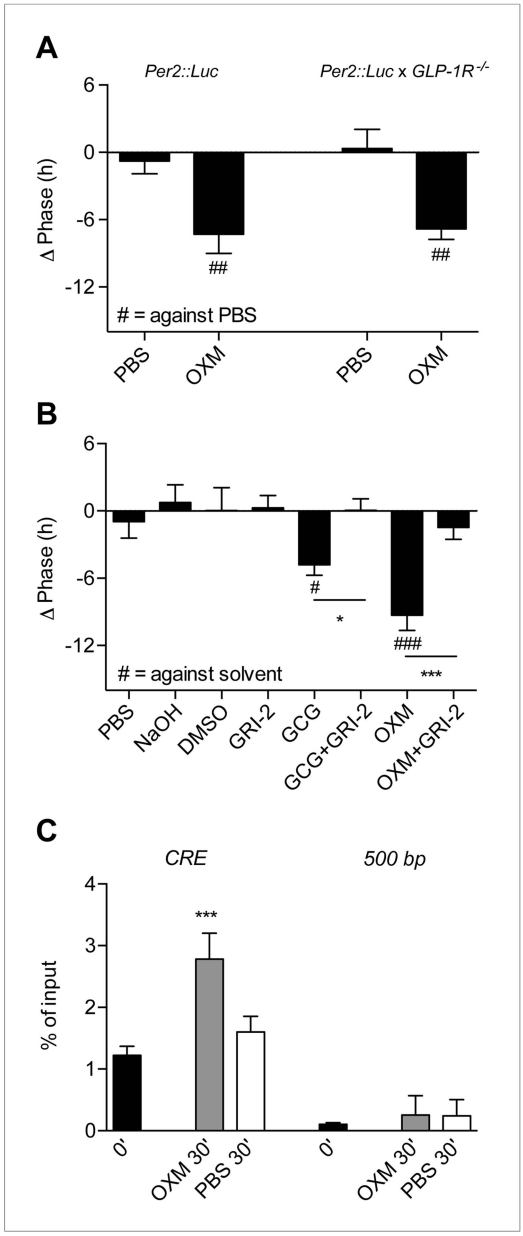

Figure 2. Glucagon (GCG) receptor regulates phase resetting effects of OXM and GCG in *Per2::LUC* liver slices. (**A**) OXM-induced phase shifts in *Per2::LUC* and *Per2::LUC* x *Glp1r*$^{-/-}$ liver slices. Mann–Whitney test: ##p < 0.01 against solvent. (**B**) GCG and OXM-induced phase shifts in *Per2::LUC* slices are abolished by co-treatment with GRI-2. One-way ANOVA with Bonferroni post-test: p < 0.05; ###p < 0.001 against solvent; *p < 0.05; ***p < 0.001. Data are presented as mean ± S.E.M. (n = 8); F(7, 56) = 7.314. (**C**) OXM treatment promotes binding of CREB to CRE elements at the *Per1* gene promoter. One-way ANOVA with Bonferroni post-test: ***p < 0.001 against 0′. Data are presented as mean ± S.E.M. (n = 5; F(5, 24) = 22.2).

DOI: 10.7554/eLife.06253.006

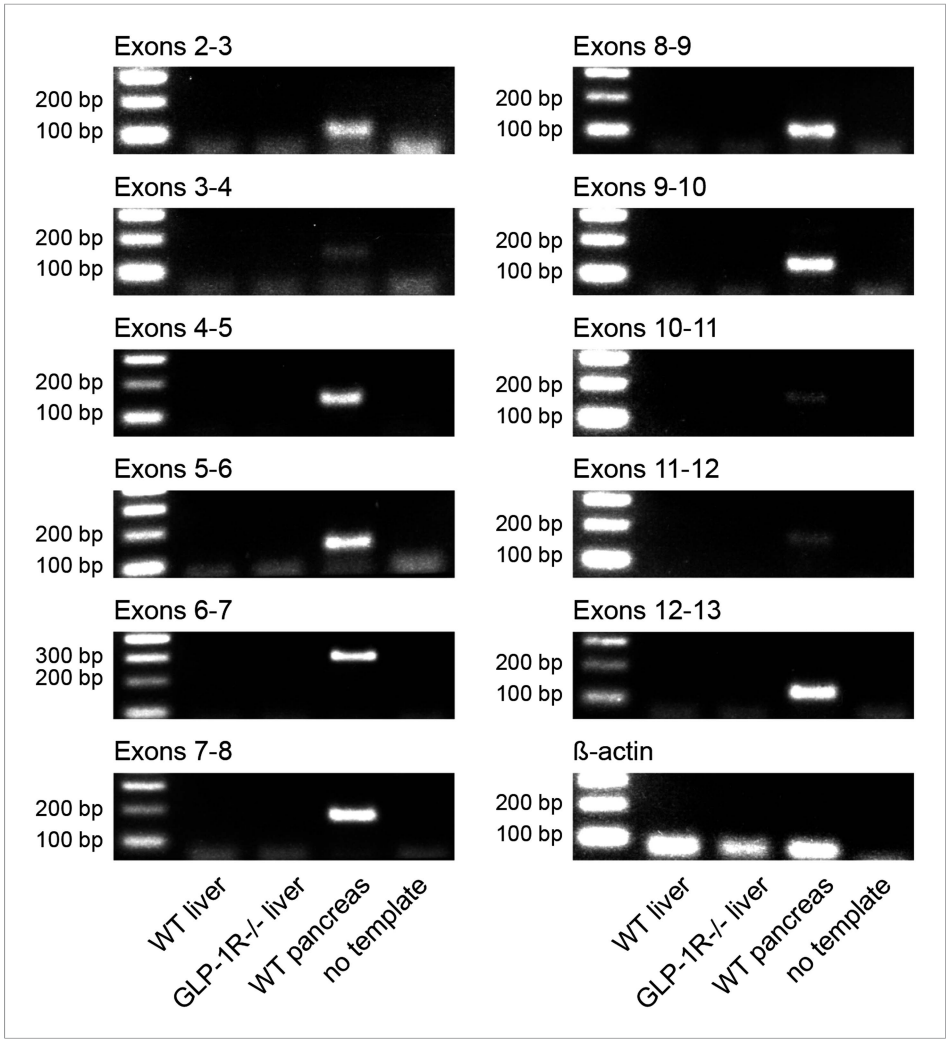

Figure 2—figure supplement 1. Absence of *Glp1r* transcripts in mouse liver. RT-PCR with different primer sets targeting all annotated coding exons of the murine *Glp1r* gene. Exon 1 was not tested, as it mainly contains non-coding poly-C- and poly-G-rich sequences, which precludes specific primer design. cDNA preparations from wild-type livers were tested (lane 2). Wild-type pancreas cDNA was chosen as positive (lane 4) and liver cDNA from *Glp1r*-deficient mice and water as negative controls (lanes 3 and 5). Lane 1: 100-bp DNA ladder.

DOI: 10.7554/eLife.06253.007

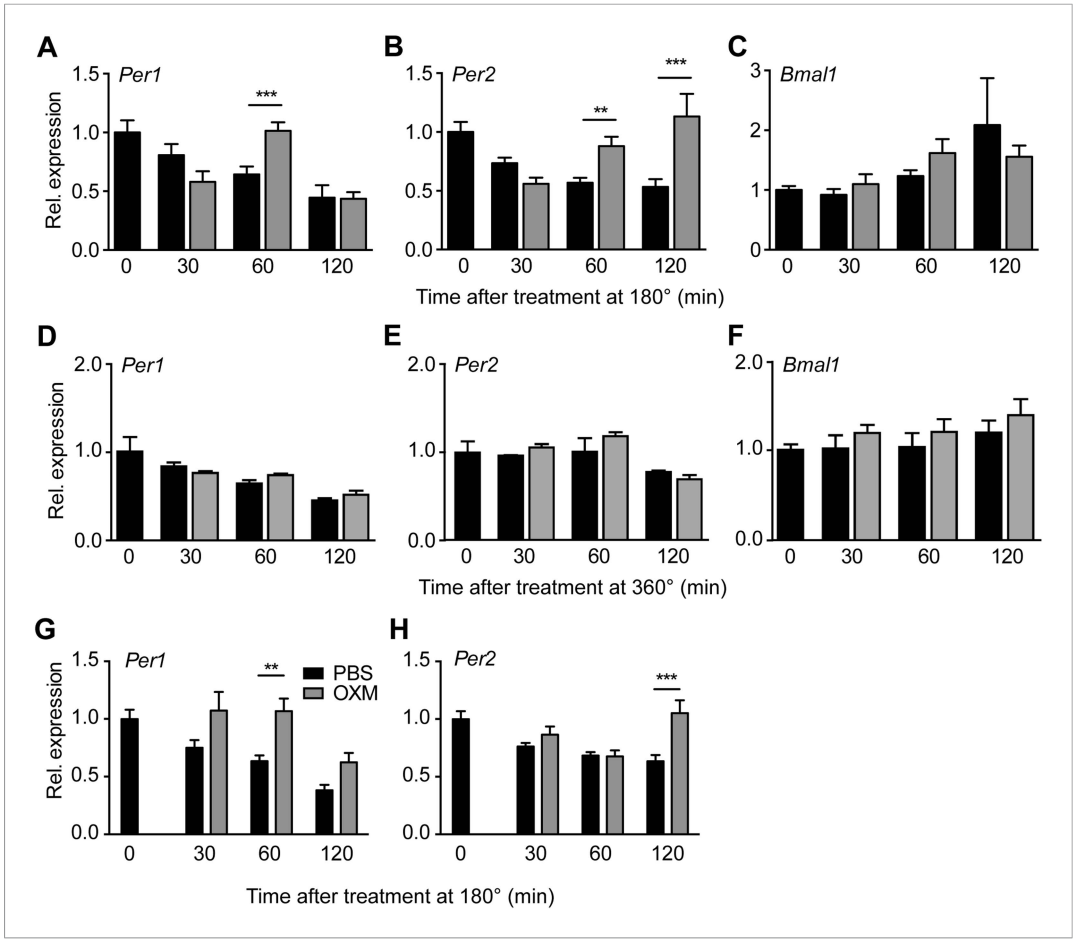

Figure 3. OXM treatment induces *Per1/2* expression in organotypic liver slices. (**A**–**C**) WT liver slices were treated with OXM (grey) or vehicle (PBS; black) at 180˚ and analyzed for clock gene expression of *Per1* (**A**; factor treatment F (1, 40) = 0.785; time F(3, 40) = 34.95; interaction F(3, 40) = 16.33), *Per2* (**B**; factor treatment F(1, 40) = 24.02; time F(3, 40) = 29.4; interaction F(3, 40) = 38.38), and *Bmal1* (**C**; factor treatment F(1, 40) = 0.108; time F(3, 40) = 17.39; interaction F(3, 40) = 3.607) by qPCR. (**D**–**F**) WT liver slices were treated with OXM (grey) or PBS (black) at 360˚ and analyzed for expression of *Per1* (**D**; factor treatment F(1, 40) = 1.179; time F(3, 40) = 36.33; interaction F(3, 40) = 1.349), *Per2* (**E**; factor treatment F(1, 40) = 5.757; time F(3, 40) = 13.57; interaction F(3, 40) = 1.135), and *Bmal1* (**F**; factor treatment F(1, 40) = 4.112; time F(3, 40) = 8.788; interaction F(3, 40) = 0.491) by qPCR. (**G** and **H**) OXM-induced *Per1/2* expression is retained in *Glp1r*$^{-/-}$ liver slices. *Per1*: factor treatment F(1, 42) = 8.48; time F(2, 42) = 10.95; interaction F(2, 42) = 0.525. *Per2*: factor treatment F(1, 42) = 10.5; time F(2, 42) = 3.662; interaction F(2, 42) = 5.845. *Glp1r*$^{-/-}$ liver slices were treated as described for WT above. Data are presented as mean ± S.E.M. (n = 6 for WT and 8 for *Glp1r*$^{-/-}$). Two-way ANOVA with Bonferroni post-test: **p < 0.01; ***p < 0.001.

DOI: 10.7554/eLife.06253.008

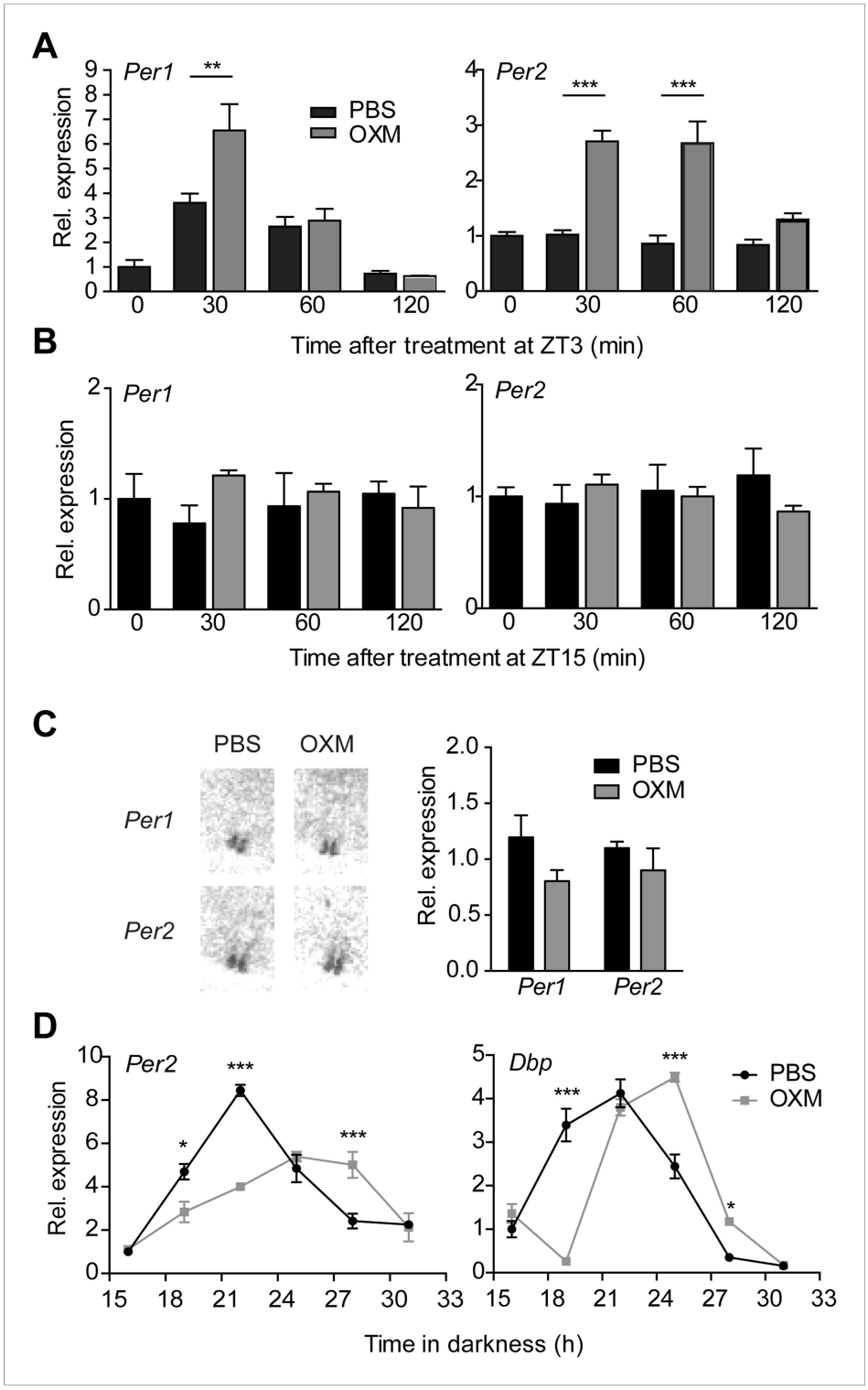

Figure 4. OXM treatment induces *Per1/2* expression and resets the liver circadian clock in vivo. (**A** and **B**) Hepatic *Per* gene expression after OXM (grey) or vehicle (PBS; black) *i.v.* injection at ZT3 (**A**) and ZT15 (**B**). ZT3: *Per1*: factor treatment F(1, 24) = 5.695; time F(2, 24) = 34.74; interaction F(2, 24) = 4.965; *Per2*: factor treatment F(1, 24) = 64.84; time F(2, 24) = 9.381; interaction F(2, 24) = 6.915. ZT15: *Per1*: factor treatment F(1, 12) = 1.096; time F(2, 12) = 0.005; interaction F(2, 12) = 1.367; *Per2*: factor treatment F(1, 24) = 0.255; time F(2, 24) = 0.001; interaction F(2, 24) = 1.172. (**C**) Suprachiasmatic nucleus (SCN) signal after in situ hybridization (ISH) of brain sections with ^{35}S-labelled antisense probes for *Per1/2* 30 min after OXM/PBS treatment at ZT3 in the same animals used in (**A**). Left panel: representative

Figure 4. continued on next page

Figure 4. Continued

autoradiograph scans containing the SCN; right panel: quantification of the ISH. (**D**) Resetting of *Per2* and *Dbp* rhythms in livers of wild-type mice after an *i.p.* injection of either OXM (grey) or vehicle (PBS; black) after 12-hr darkness; *Per2*: factor treatment $F(1, 24) = 5.531$; time $F(5, 24) = 46.37$; interaction $F(5, 24) = 18.71$. *Dbp*: factor treatment $F(1, 24) = 0.094$; time $F(5, 24) = 119.2$; interaction $F(5, 24) = 38.58$. All data are presented as mean ± S.E.M. (n = 3–5). **A**, **B**, and **D**: two-way ANOVA with Bonferroni post-test: *$p < 0.05$, **$p < 0.01$; ***$p < 0.001$; **C**: Mann–Whitney test.

DOI: 10.7554/eLife.06253.009

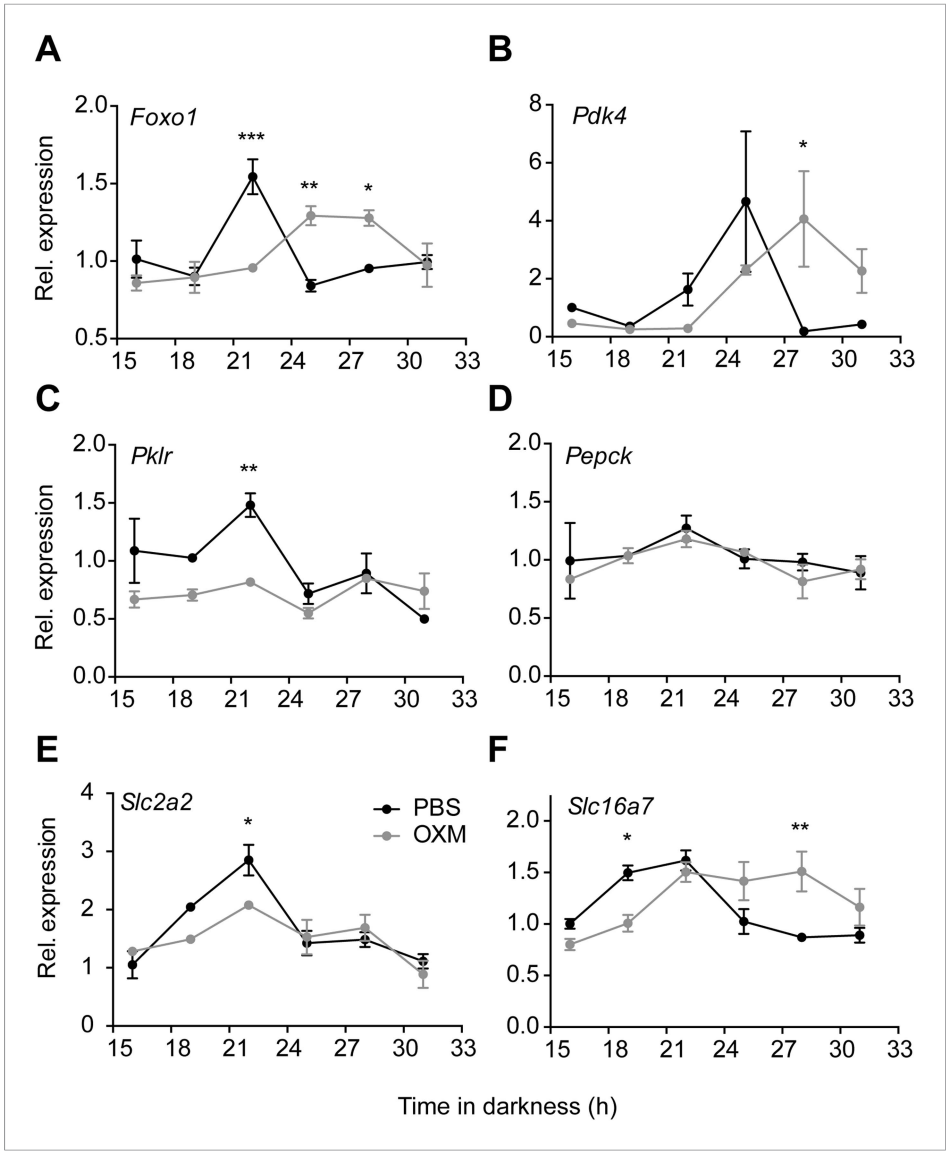

Figure 5. OXM treatment modulates diurnal expression profile of hepatic genes involved in liver carbohydrate metabolism. (**A**–**F**) Relative gene expression of *Foxo1* (**A**; factor treatment F(1, 24) = 0.001, time F(5, 24) = 5.547, interaction F(5, 24) = 11.13), *Pdk4* (**B**; factor treatment F(1, 24) = 0.197, time F(5, 24) = 3.35, interaction F(5, 24) = 3.247), *Pklr* (**C**; factor treatment F(1, 24) = 11.63, time F(5, 24) = 5.61, interaction F(5, 24) = 3.61), *Pepck* (**D**; factor treatment F(1, 24) = 0.574, time F(5, 24) = 2.043, interaction F(5, 24) = 0.299), the glucose transporter *Slc2a2* (**E**; factor treatment F(1, 24) = 2.582, time F(5, 24) = 15.98, interaction F(5, 24) = 2.642) and the pyruvate transporter *Slc16a7* (**F**; factor treatment F(1, 24) = 1.539, time F(5, 24) = 7.472, interaction F(5, 24) = 6.586) after *i.p.* administration of either OXM (grey) or vehicle (PBS; black) after 12 hr in darkness. Data are presented as mean ± S.E.M. (n = 4). Two-way ANOVA with Bonferroni post-test: *p < 0.05, **p < 0.01; ***p < 0.001.

DOI: 10.7554/eLife.06253.010

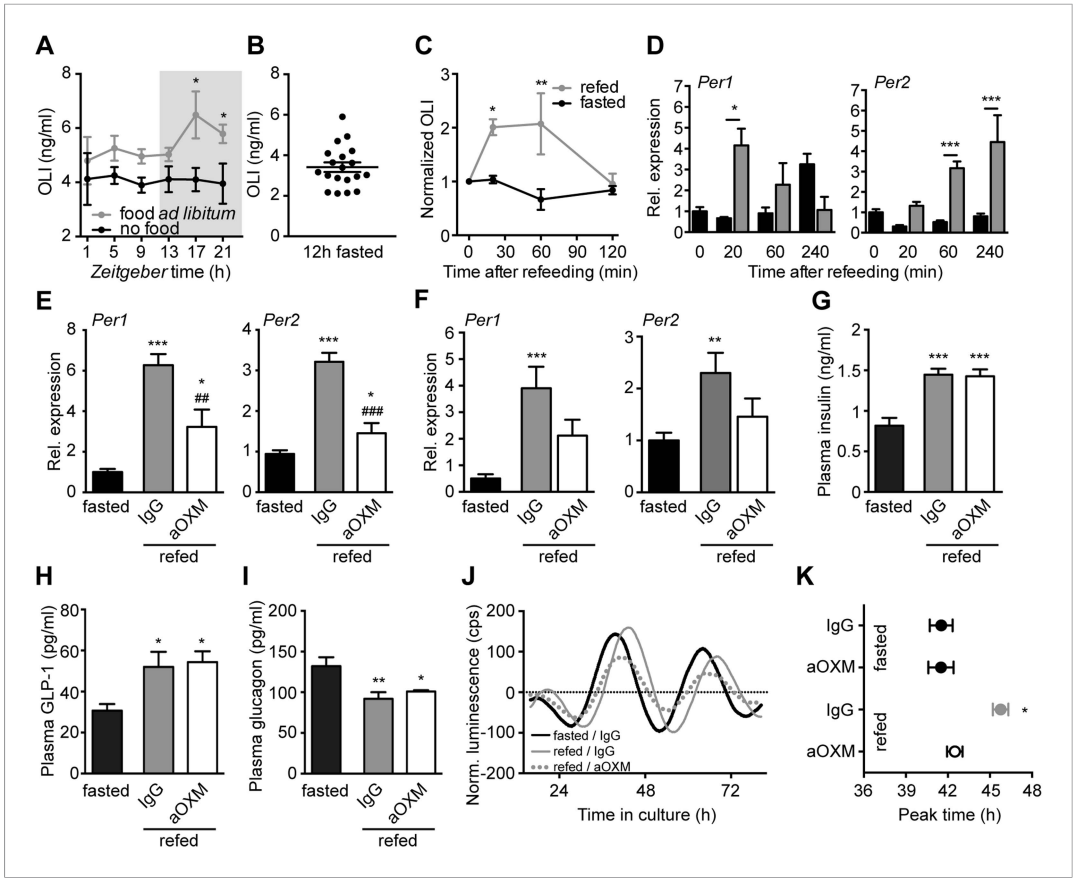

Figure 6. Endogenous OXM signaling regulates food intake-mediated resetting of the liver circadian clock. (**A**) Plasma oxyntomodulin-like immunoreactivity (OLI) diurnal profiles under ad libitum food and fasting conditions. Data are presented as mean ± S.E.M (n = 6); factor time F(5, 60) = 0.628, feeding condition F(1, 60) = 15.37, interaction F(5, 60) = 0.638. Grey shading indicates the dark phase. (**B**) OLI levels show high individual variations in mice after 12 hr of food deprivation (ZT13-1). (**C**) Plasma OLI (normalized to individual fasting levels) after refeeding (grey line) or under continuous starving (black line); factor time F(3, 21) = 3.544, feeding condition F(1, 21) = 15.82, interaction F(3, 21) = 4.717. (**D**) Liver *Per1/2* induction following fasting-refeeding determined by qPCR; *Per1*: factor time F(3, 25) = 0.454, feeding condition F(1, 25) = 1.376, interaction F(3, 25) = 4.453; *Per2*: factor time F(3, 25) = 6.938, feeding condition F(1, 25) = 38.48, interaction F(3, 25) = 3.767. (**E**) WT and (**F**) *Glp1r*$^{-/-}$ liver *Per1/2* expression after fasting-refeeding with control IgG injection (grey) or OXM immuno-neutralization by *anti*-OXM IgG (aOXM) injection at ZT0; WT: *Per1*: F(2, 12) = 71.76, *Per2*: F(2, 12) = 47.41; *Glp1r*$^{-/-}$: *Per1* F(2, 12) = 11.51, *Per2*: F(2, 12) = 5.585. (**G**–**I**) Treatment with *anti*-OXM IgG does not affect postprandial regulation of insulin, GLP-1, and GCG. Plasma levels of insulin (**G**; F(2, 12) = 17.44), GLP-1 (**H**; F(2, 12) = 5.563), and GCG (**I**; F(2, 12) = 7.128) after fasting-refeeding with control IgG injection (grey) or OXM immuno-neutralization by *anti*-OXM IgG (aOXM) treatment at ZT0. One- (**E**–**I**) or two-way ANOVA (**A**, **C**, **D**) with Bonferroni post-test: *p < 0.05; **p < 0.01; ***p < 0.001 against fasted; ##p < 0.01; ###p < 0.001 against IgG. Data are presented as mean ± S.E.M (n = 5). (**J** and **K**) Liver PER2::LUC rhythms after fasting-refeeding with control IgG or αOXM administration. (**J**) Representative luminescence traces. (**K**) Comparison of phases (second peak in culture) after refeeding and/or *anti*-OXM treatment (Data are presented as mean ± S.E.M (n = 4 mice per condition, an average of 3 slice preparations of each mouse were used); two-way ANOVA with Bonferroni post-test: *p < 0.05 against fasted; factor treatment F(1, 12) = 5.127, feeding condition F(1, 12) = 13.02, interaction F(1, 12) = 5.044).

DOI: 10.7554/eLife.06253.011

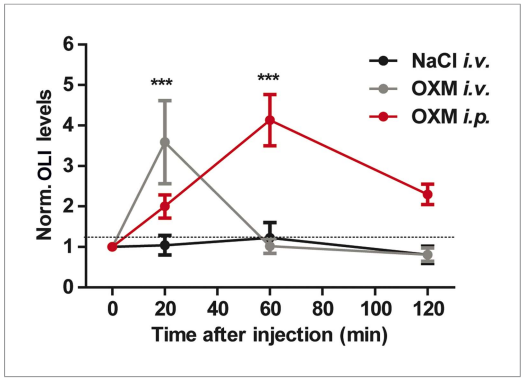

Figure 6—figure supplement 1. Time course of OLI plasma levels after OXM injection. Time course of OLI appearance in plasma following *i.v.* (4 μg) or *i.p.* (25 μg) injections of OXM. OLI plasma level changes are expressed relative to starving levels (0 min) for each individual. Data are presented as mean ± SEM (n = 5). 2-way ANOVA with Bonferroni post-test: ***$p < 0.001$; factor treatment $F(2, 48) = 9.014$, feeding condition $F(3, 48) = 4.95$, interaction $F(6, 48) = 5.698$.

DOI: 10.7554/eLife.06253.013